CHEMISTRY

A metal-free blue chromophore derived from plant pigments

B. C. Freitas-Dörr[1], C. O. Machado[1], A. C. Pinheiro[1], A. B. Fernandes[1], F. A. Dörr[2], E. Pinto[2], M. Lopes-Ferreira[3], M. Abdellah[4,5], J. Sá[4,6], L. C. Russo[7], F. L. Forti[7], L. C. P. Gonçalves[1], E. L. Bastos[1]*

Blue natural pigments are rare, especially among plants. However, flowering species that evolved to attract Hymenoptera pollinators are colored by blue anthocyanin-metal complexes. Plants lacking anthocyanins are pigmented by betalains but are unable to produce blue hues. By extending the π-system of betalains, we designed a photostable and metal-free blue dye named BeetBlue that did not show toxicity to human hepatic and retinal pigment epithelial cells and does not affect zebrafish embryonal development. This chiral dye can be conveniently synthesized from betalamic acid obtained from hydrolyzed red beetroot juice or by enzymatic oxidation of L-dopa. BeetBlue is blue in the solid form and in solution of acidified polar molecular solvents, including water. Its capacity to dye natural matrices makes BeetBlue the prototype of a new class of low-cost bioinspired chromophores suitable for a myriad of applications requiring a blue hue.

INTRODUCTION

The notion that natural means healthy and safe to consume has increased the demand for natural color ingredients for food, cosmetics, and drugs. However, finding high-performance and economically viable natural colorants is difficult, especially for blue hues (*1*). Blue mineral pigments inspired artists to represent the blue sky and waters, but despite their usual high stability, these materials are often expensive and contain toxic metal cations that limit their broad application. The visual exuberance of animals with blue structures frequently originates from coherent light scattering. Examples include the blue wings of the jaybird (*Cyanocitta cristata* L.) and morpho butterflies (*Morpho* spp. L.), the feather barbs of male Indian peacock (*Pavo cristatus* L.), and the hairs of the blue carpenter bee (*Xylocopa caerulea* F.) (*2*). Bioluminescence can also make animals and microorganisms look blue, at the cost of the adenosine triphosphate–fueled enzymatic oxidation of luciferins (*3*). Since the natural blue color of most living organisms cannot be easily harnessed (*4*–*7*), there is a quest for new blue chromophores that could be converted into colored commodities (*8*, *9*).

Highly evolved flower species have blue-colored petals that attract Hymenoptera pollinators, such as bees and wasps, which are red colorblind (*10*). Blue hydrangea (*Hydrangea macrophylla* L.), cornflower (*Centaurea cyanus* L.), morning glory (*Ipomoea tricolor* Cav.), *speedwell* (*Veronica* spp. L.), and several other species are pigmented by blue metal-anthocyanin supramolecular complexes and polyacylated anthocyanins (*11*). These blue pigments are highly unstable ex vivo, making their characterization and application difficult (*12*, *13*).

In most plants of the order Caryophyllales, anthocyanins are replaced by red-violet and yellow-orange betalains (*14*, *15*), which are safe for human consumption (*6*, *16*). Red beetroots are rich in betanin, an antioxidant betalain widely used as a food color additive (EFSA E162/FDA 73.40) (*16*), a redox mediator (*17*, *18*), and a renewable source of betalamic acid, the chiral precursor of betalains in vitro and in vivo (*19*, *20*). Although there are no blue natural betalains, derivatives with an extended π-system and reduced excitation gap would show blue hues. However, the C═N coupling of betalamic acid and nitrogen nucleophiles, such as amines and amino acids (*20*), restrains betalains to the 1,7-diazaheptamethinium chromophore, which is not blue.

Here, we report the synthesis and properties of BeetBlue, a bioinspired metal-free dye. Despite sharing some of the characteristics of betalains, BeetBlue is the first example of a quasibetalain, a new class of betalamic acid derivatives with extended π-conjugation. The 1,11-diazaundecamethinium chromophore of BeetBlue is formed by the expeditious acid-catalyzed coupling of betalamic acid and the carbon nucleophile 2,4-dimethylpyrrole. This dye is nontoxic for human hepatic and retinal pigment epithelial cell lines or zebrafish and does not produce singlet oxygen upon photoexcitation. It shows high solubility in polar solvents including water and imparts color to different natural matrices allowing myriad applications.

RESULTS AND DISCUSSION

Semisynthesis and structural characterization of BeetBlue

BeetBlue was obtained by the irreversible dehydrative C─C coupling of betalamic acid (HBt) and 2,4-dimethylpyrrole (2,4-dmp) in acidified ethyl acetate (Fig. 1A and movie S1). The product was isolated in 70% yield, which is three times higher than that reported for the semisynthesis of betalains (*21*, *22*). Betalamic acid can be extracted from base-hydrolyzed beetroot juice (*20*, *23*) or prepared by the enzymatic oxidation of L-dopa (*24*–*27*).

Nuclear magnetic resonance (NMR) analyses and quantum-mechanical gauge-independent atomic orbital (GIAO) calculations (figs. S1 to S6) show that the nucleophilic attack of C2 of 2,4-dmp on the carbonyl group of HBt forms a new C─C bond. Furthermore,

[1]Departamento de Química Fundamental, Instituto de Química, Universidade de São Paulo, 05508-000 São Paulo, SP, Brazil. [2]Departamento de Análises Clínicas e Toxicológicas, Faculdade de Ciências Farmacêuticas, Universidade de São Paulo, 05508-000 São Paulo, SP, Brazil. [3]Immunoregulation Unit of the Special Laboratory of Applied Toxinology (Center for Toxins, Immune-Response and Cell Signaling/CEPID/FAPESP), Butantan Institute, 05503-900 São Paulo, SP, Brazil. [4]Physical Chemistry Division, Department of Chemistry, Ångström Laboratory, Uppsala University, 75120 Uppsala, Sweden. [5]Department of Chemistry, Qena Faculty of Science, South Valley University, 83523 Qena, Egypt. [6]Institute of Physical Chemistry, Polish Academy of Sciences, 01-224 Warsaw, Poland. [7]Departamento de Bioquímica, Instituto de Química, Universidade de São Paulo, 05508-000 São Paulo, SP, Brazil.
*Corresponding author. Email: elbastos@iq.usp.br

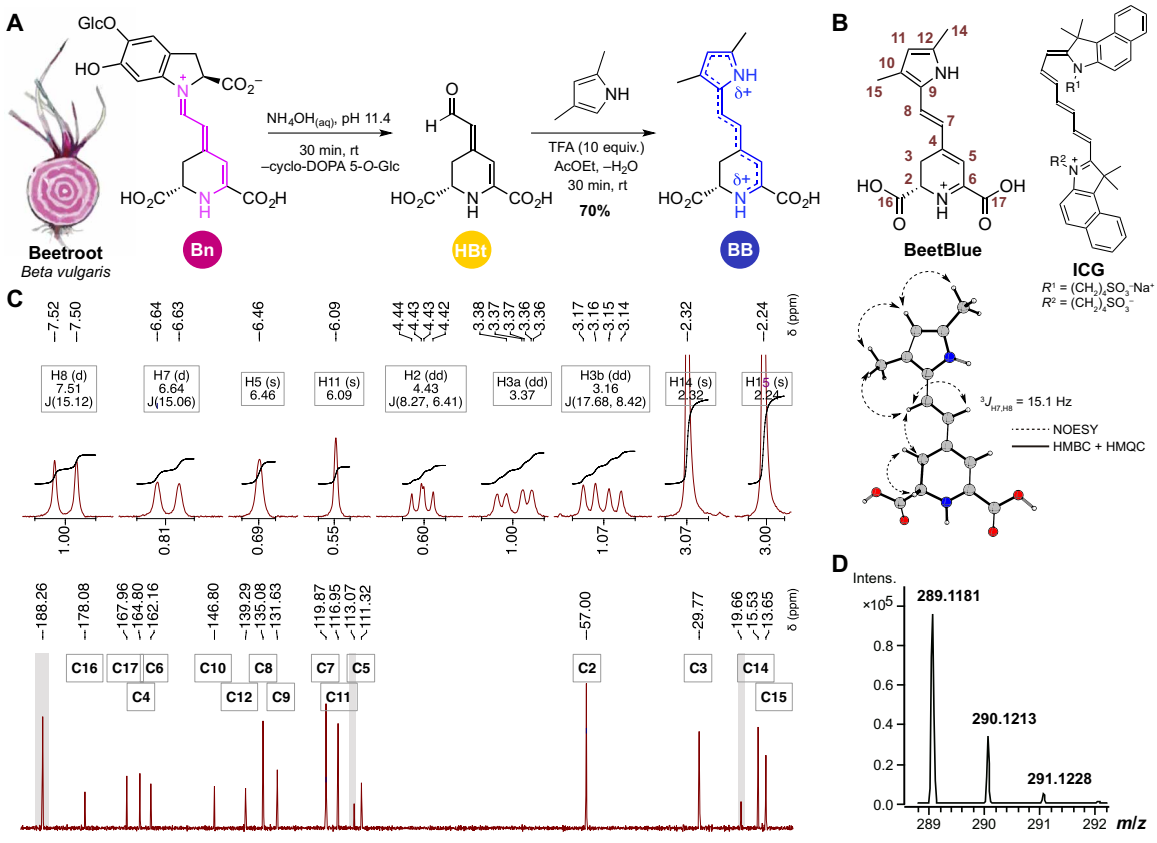

Fig. 1. Semisynthesis and spectroscopic data of BeetBlue. (**A**) Acid-catalyzed coupling of betalamic acid (HBt) and 2,4-dimethylpyrrole (2,4-dmp) in ethyl acetate. The reaction, which takes less than 30 min to complete, is performed at room temperature (rt) under air, and the product can be purified by flash gel permeation chromatography using water as eluent. TFA, trifluoroacetic acid; BB, BeetBlue; Bn, betanin. (**B**) Chemical structures of BeetBlue and indocyanine green (ICG), atom numbering, and density functional theory (DFT)–optimized geometry of BeetBlue. NOESY, nuclear Overhauser effect spectroscopy; HMQC, heteronuclear multiple-quantum coherence; HSQC, heteronuclear single-quantum coherence. (**C**) ^{1}H and ^{13}C NMR spectra of BeetBlue (13 mM, 800 MHz/200 MHz, D_2O at 288 K). (**D**) High-resolution mass spectrum of BeetBlue; *m/z* 289.1181, $[M + H]^+$.

these results increase knowledge of the structure of betalamic acid derivatives since their ^{13}C NMR and two-dimensional (2D) NMR spectra have been scarcely reported (*28*, *29*). The π-conjugation of the resulting diazapolymethine system is extended compared to that of betalains, resembling the chromophore of the widely used dye indocyanine green (ICG) (Fig. 1B). No evidence was found for the presence of a hydrogen atom at the α-position of the pyrrole ring, although the α carbon atoms (C9 and C12) were detected in the ^{13}C NMR spectrum (Fig. 1C). The large coupling constant between H7 and H8 ($^{3}J_{H7,H8}$ = 15.2 Hz) is in the expected range for a *trans* alkene (14 to 16 Hz) but is larger than the values reported for betalains (roughly 10 to 12 Hz) (*28*), indicating C—C bond formation.

High-resolution mass spectral analysis of the blue-colored product (Fig. 1D) exhibited a signal at mass/charge ratio (*m*/*z*) 289.1181 corresponding to the $[M + H]^+$ ion of BeetBlue (exact mass, 289.1183 Da). The fragmentation of this ion occurs via single and double decarboxylation leading to signals at *m*/*z* 245.1250 and 201.1384, respectively (fig. S7). The fragment at *m*/*z* 108.0800 results from double decarboxylation and loss of the pyrrolic portion of BeetBlue, supporting the presence of the C—C bond.

Color properties

Natural betalains have yellow-orange or red-violet color depending on the electronic properties of the substituents attached to the imine/iminium (N9) nitrogen atom. The extended π-conjugation of the 1,11-diazaundecamethinium chromophore of BeetBlue induces a redshift of both its absorption and fluorescence spectra in water relative to the standard betalains betanin and indicaxanthin (Fig. 2A). The maximum molar absorption coefficient (ε) of BeetBlue at 582 nm is 54,000 liter mol^{-1} cm^{-1} (fig. S8), which is within the 40,000 to 70,000 liter mol^{-1} cm^{-1} range typical of betalains (*30*).

The spectrophotometric titration of BeetBlue reveals that its color does not depend on the pH within the range of 3 to 8 (Fig. 2B). It is noticeable that the protonation of the carboxylic acid moieties [pK_a (the negative logarithm of the acid dissociation constant, K_a) = 2.9] under very acidic conditions redshifts the absorption spectra compared to neutral conditions. However, deprotonation of the N1 atom of the 2,3-dihydropyridine ring under alkaline conditions (pK_a = 9.6) affects charge distribution in the chromophore, reversibly changing BeetBlue's color from blue to yellow (fig. S9). This reversible behavior differs from that of natural betalains, which undergo further decomposition in alkaline media.

Blue hues of dyes often vanish or alter under acidic conditions, and molar absorption coefficients are quite low (*5*). That is not the case for BeetBlue, which maintains its blue color in a variety of acidified solvents (Fig. 2C) and becomes bluer in organic solvents such as dimethyl sulfoxide (DMSO) and trifluoroethanol (TFE). This minimal solvatochromism indicates that the hydrogen bond donation capacity of the solvent does not affect the charge distribution of the fully protonated form of BeetBlue. The perceived color of each solution

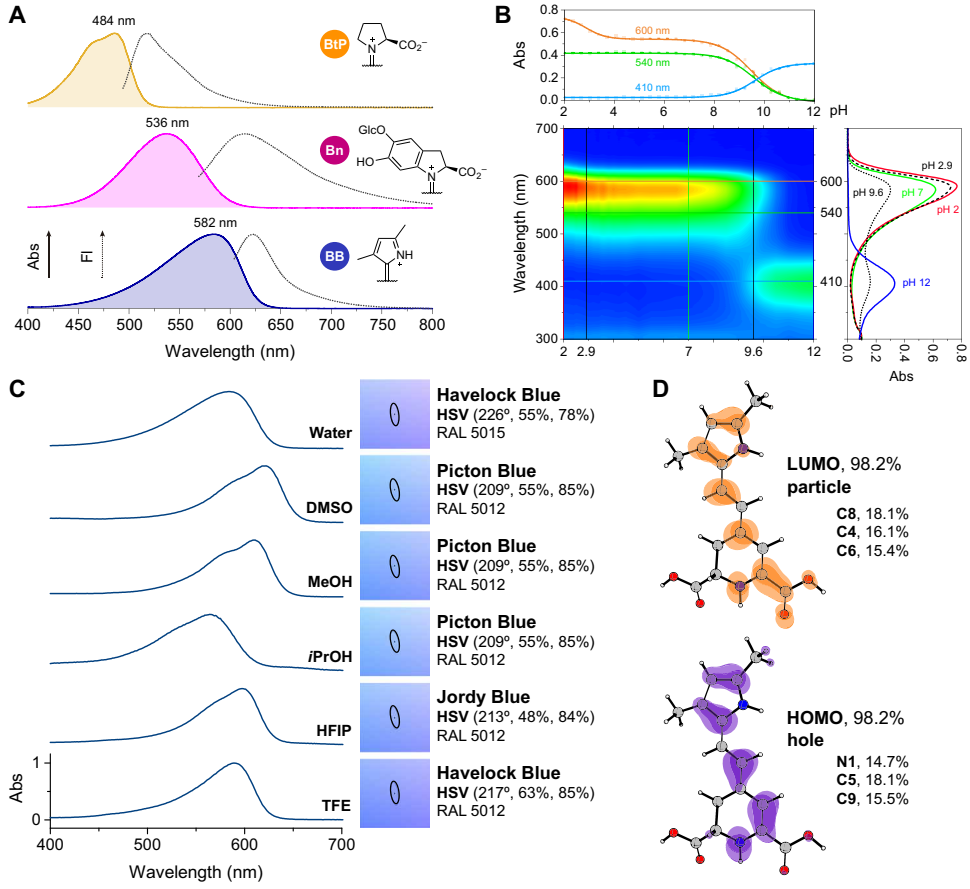

Fig. 2. Characterization of the electronic and physicochemical properties of BeetBlue in solution. (**A**) Comparison of the normalized ultraviolet-visible (UV-Vis) (filled) and fluorescence spectra of BeetBlue, betanin, and indicaxanthin (BtP) in water. FI, fluorescence. (**B**) Titration of BeetBlue within the range of pH 2 to pH 12 using Britton-Robinson buffer (40 mM). The top projection shows the dependence of the absorption at selected wavelengths on the pH; lines are a nonlinear fit of a sigmoidal function to the data for determining the pK_a values. The right projection shows the absorption spectra at selected pHs (2, 2.9 [pK_{a1}], 7, 9.6 [pK_{a2}], and 12). For reference, the pK_as of the carboxylic acid groups of betanin and indicaxanthin are roughly 3.5 (*23*). (**C**) Absorption spectra, magnification of the CIELUV (CIE 1976 L*, u*, v* color space) chromaticity diagram (2015 D65/10°), and MacAdam ellipses of diluted solutions of BeetBlue in acidified (0.1 mM *p*-toluenesulfonic acid) polar molecular solvents. Values of RAL (Reichs-Ausschuß für Lieferbedingungen) color matching system and HSV (hue, saturation, value) and color names are given for referencing purposes. MeOH, acidified methanol; DMSO, dimethyl sulfoxide; TFE, trifluoroethanol; *i*PrOH, isopropanol; HFIP, hexafluoro-2-propanol. (**D**) Natural transition orbitals (NTOs) of BeetBlue at the SMD/PBE0/6-31+G(d,p)// SMD/B3LYP/6-31+G(d,p) level (isovalue, 0.002 e); orbital and relevant atom contribution to hole and particle states. LUMO, lowest unoccupied molecular orbital.

is shown at the center of the magnified region of the chromaticity diagram; colors that are indistinguishable to the human eye are shown in the MacAdam ellipses (Fig. 2C) (*31*). Natural transition orbital (NTO) analysis shows that both the charge distribution of the ground state and the locally excited state are contained within the 1,11-diazaundecamethinium system, being shifted from the α,β-unsaturated enamine system formed by the atoms N1, C5, and C9 to the polymethine system (C4, C6, and C8) (Fig. 2D). The carboxylic acid moiety attached to the sp^2 carbon atom of the 2,3-dihydropyridine ring participates in the electronic transition, explaining the effect of its protonation state on the absorption spectrum of BeetBlue.

Toxicity and potential application

The application of new dyes requires safety assessment. BeetBlue was tested for cytotoxicity to human hepatic and retinal pigment epithelial cells in culture and for in vivo toxicity to zebrafish embryos (*Danio rerio* Hamilton, 1822). The 3-(4,5-dimethylthiazol-2-yl)-2,5-diphenyltetrazolium bromide (MTT) assay was used to determine the viability of the immortalized human hepatic cell lines Huh-7, Hep-G2, and HepaRG treated with BeetBlue for 8 hours (Fig. 3A). Cells incubated with the dye (0.1 mM to 1 nM) remained 100% viable, and 1 mM BeetBlue was required to reduce cell viability by 20 to 30%. Although these cell lines have been widely used in toxicological studies (*32*), hepatocyte-like HepaRG cells express a large set of liver-specific functions and, therefore, were selected to investigate the genotoxicity of BeetBlue. Cells were treated with the dye (10 μM) for up to 8 hours, and DNA fragmentation did not differ from the untreated negative control, as measured by single-cell gel electrophoresis (Comet assay; Fig. 3B). The cytotoxicity of BeetBlue was also verified by determining the viability of ARPE-19 cells using 7-aminoactinomycin D (7-AAD) as the fluorescent marker for membrane integrity (Fig. 3C). This human pigment epithelial cell line has been used as a model to investigate the toxicity and phototoxicity of dyes due to its response to factors related to photoinduced macular degeneration, including photosensitized singlet oxygen formation (*33*). After incubation with the dye (10 μM) for 24 hours, a single population of cells is found, in contrast with the at least two distinct cell populations observed when cells were incubated with

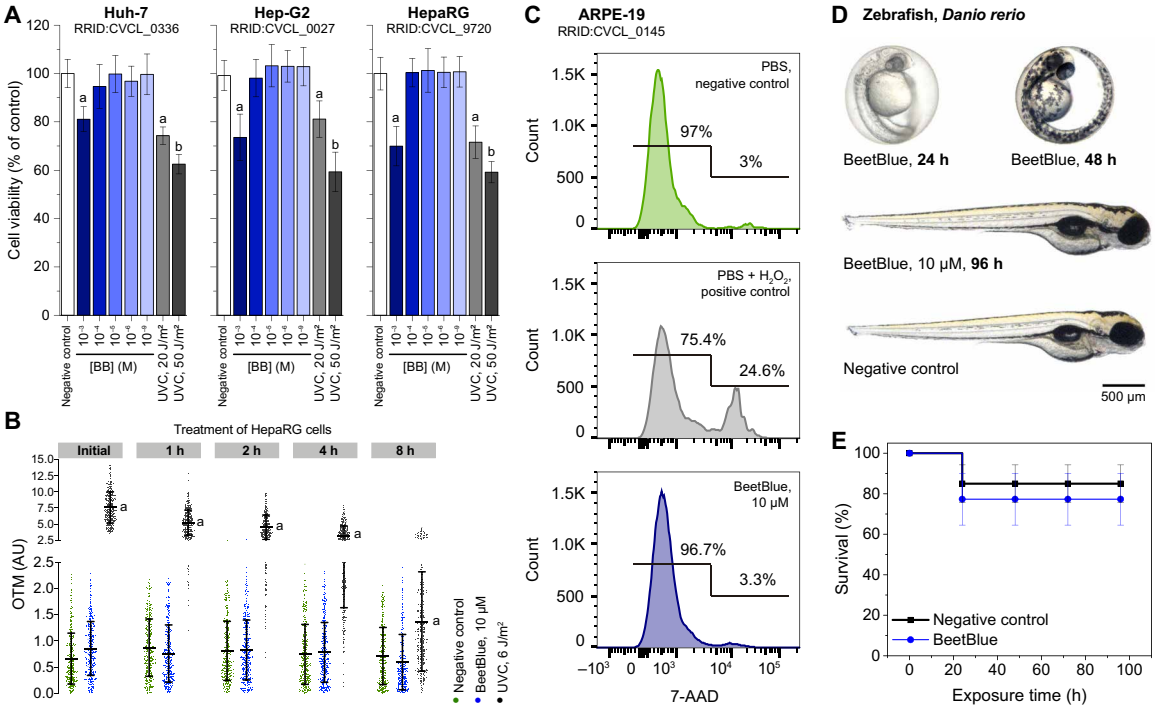

Fig. 3. Toxicological analyses of BeetBlue. (**A**) Viability of Huh-7, Hep-G2, and HepaRG cells treated with BeetBlue [1 mM to 1 nM, 8 hours, in phosphate-buffered saline (PBS)] measured by using the MTT assay. Negative controls were carried out using PBS; cells irradiated with UVC light (20 and 50 J/m^2) were used as positive controls. The Research Resource Identifiers (RRIDs) for the cell lines are given for convenience. The letters indicate statistical significance ($P < 0.05$, one-way ANOVA, Tukey's post hoc test, $N > 10$). (**B**) Quantitative Comet assay results in HepaRG cells treated with BeetBlue (10 µM) for up to 8 hours. Cells irradiated with UVC light (6 J/m^2) were used as positive controls. DNA fragmentation was expressed as olive tail moment (OTM), viz., the product of the tail length and the fraction of total DNA in the tail. Untreated cells were used as a negative control group. AU, arbitrary units. (**C**) Viability of ARPE-19 cells (1×10^{-6} cells) incubated with PBS, hydrogen peroxide (50 mM, 5 hours, in PBS), or BeetBlue (10 µM, 24 hours, in PBS) measured by flow cytometry; percentages show the relative populations. (**D**) Aspect of zebrafish larvae in culture for 4 days in the presence of 10 µM BeetBlue versus negative control. (**E**) Survival of zebrafish in the presence and absence of BeetBlue (10 µM) for 4 days; $N = 16$.

50 mM hydrogen peroxide for 5 hours (Fig. 3C). The fish embryo acute toxicity test was performed according to the guidelines of the Organization for Economic Cooperation and Development (OECD) (*34*). To test the effect of BeetBlue on the development of zebrafish embryos, we kept the animals in culture in E2 medium in the presence of the dye (10 µM) for 4 days. The morphology of the zebrafish larvae during growth in the presence of BeetBlue is identical to that of the negative control in the absence of the dye (Fig. 3D). The death of embryos and larvae incubated with BeetBlue along the experiment does not differ from the negative control (Fig. 3E).

The toxicity of dyes is often related to their ability to produce singlet oxygen, which has been found to promote cell damage and death (*35*). Dyes able to undergo efficient intersystem crossing (ISC) from the singlet-excited state to the triplet manifold can transfer energy to molecular oxygen, producing singlet oxygen. Nanosecond transient absorption spectra of BeetBlue excited at 580 nm in the presence and absence of oxygen are identical (Fig. 4A). The spectra are dominated by the ground state bleaching and a positive absorption band centered at 615 nm, both with a 3.7-µs half-life, calculated from single-exponential curve fitting (fig. S10). The positive absorption could be assigned to triplet state absorption; however, the signal's insensitivity to the presence of O_2 and the lack of the characteristic chemiluminescence emission of singlet ($^1\Delta_g$) oxygen at 1270 nm suggest otherwise. Since the formation of triplet-excited states of betalains via ISC is inefficient (*36*), the most logical assignment to the positive signal centered at 615 nm is the absorption of the *cis*-form of BeetBlue formed by ultrafast photoisomerization, as observed on cyanines and rhodopsins (*37*, *38*). Laser excitation of the dye for up to 140 min at 355 or 582 nm using a power density of 2.23 and 0.45 J/s cm^2, respectively, decreased the absorption at 582 nm concomitantly with a subtle increase at around 450 nm (Fig. 4B). The accelerated photobleaching of 18.5 µM BeetBlue shows a dose-response profile and required an input fluence of 1.5 kJ/cm^2 at 582 nm or 12 kJ/cm^2 at 355 nm to halve the concentration of the dye (Fig. 4C). For comparison, 7 kJ/cm^2 is required to completely photobleach 0.2 mM ICG (*39*).

To showcase some potential applications of BeetBlue, this prototype quasibetalain was incorporated into complex matrices—such as cellulose, cotton fabric, yogurt, hair, and *Bombyx mori* silk cocoon—and encapsulated in maltodextrin (Fig. 4D). Depending on the matrix, the hue differed from that measured in aqueous solution, but under magnification, a uniform blue color distribution was observed, thus reaffirming the applicability of BeetBlue as a metal-free blue colorant.

In conclusion, a versatile new metal-free bioinspired blue chromophore was developed by extending the π-conjugations of betalains using a pyrrole. The superior stability of the prototype quasibetalain BeetBlue in solution compared to natural betalains resulted in higher preparation yields and allowed its full characterization by NMR spectroscopy and the determination of pK_a values. The precursor of BeetBlue, betalamic acid, can be obtained from renewable sources or via biotechnological production, and its coupling with 2,4-dimethylpyrrole is simple and expeditious. BeetBlue combines the advantages of the biocompatible

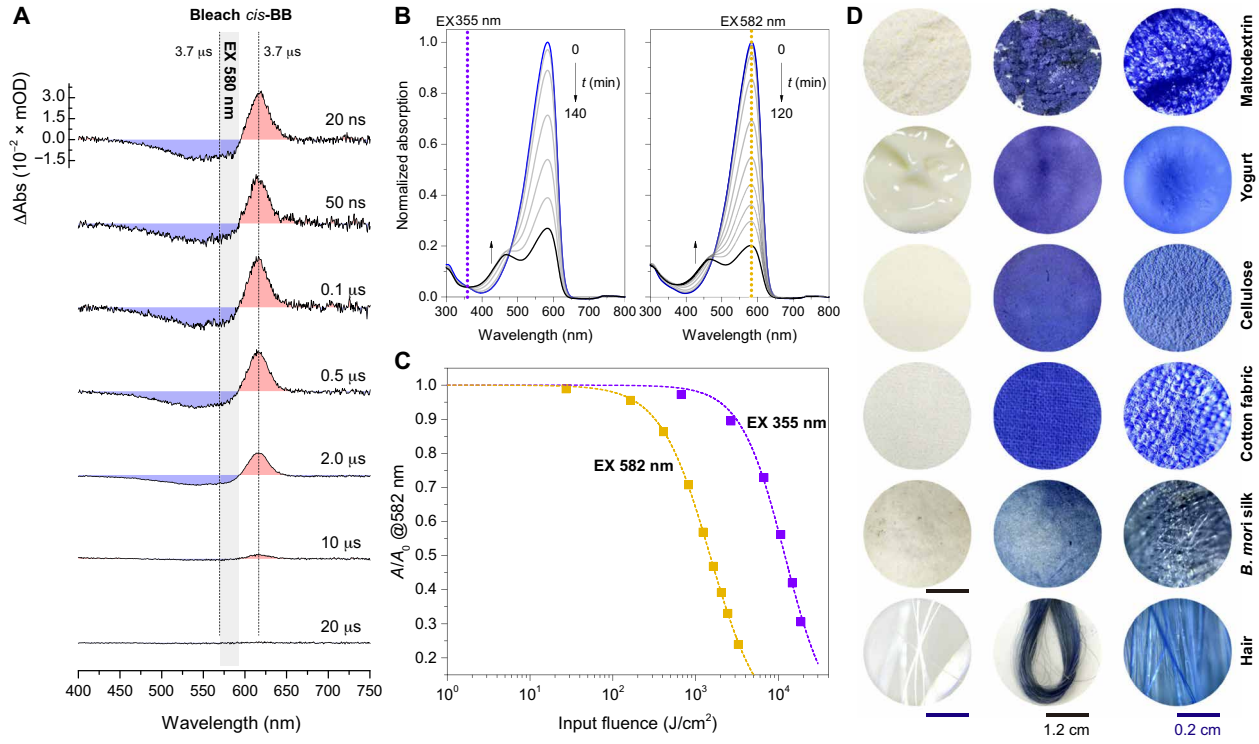

Fig. 4. Photochemical and dying properties of BeetBlue. (**A**) Nanosecond transient absorption spectra of BeetBlue in water; pump wavelength, 580 nm. mOD (milli optical density). (**B**) Effect of laser excitation at 355 nm (2.23 J/s cm^2) or 582 nm (0.45 J/s cm^2) on the absorption spectrum of an aqueous solution of BeetBlue (18.5 µM) over time. Experiments were carried out at room temperature under magnetic stirring. (**C**) Accelerated photobleaching profile of BeetBlue monitored by change in absorption at 582 nm. Solid lines are the logistic regression fit. (**D**) BeetBlue encapsulated in maltodextrin (5% w/w) or incorporated in complex matrices. Samples were illuminated with white light, and pictures were not submitted to hue adjust. The noncolored precursor materials are shown for reference.

betalainic framework with the flexibility to dye different materials. Last, quasibetalains are easy to functionalize, and thus, their properties can be tailored on demand.

MATERIALS AND METHODS

General information

All chemicals were purchased from Sigma-Aldrich and used without further purification, except as otherwise stated. Solutions were prepared using deionized water (18.2 megohm·cm at 25°C, total organic carbon (TOC) ≤ 4 parts per billion; Milli-Q, Millipore). Betalamic acid was extracted from the base-hydrolyzed juice of red beetroots using ethyl acetate and processed as described previously (*23*).

Semisynthesis of BeetBlue

In a round bottom flask equipped with a magnetic stir bar, trifluoroacetic acid (10 equiv.) or *p*-toluenesulfonic acid (10 equiv.) and 2,4-dimethylpyrrole (5 equiv.) were added to a solution of betalamic acid in ethyl acetate (10 ml; 0.6 to 6.0 mM, 6.0 to 60 µmol scale). The reaction mixture was kept under stirring at room temperature until the color of the solution changed from bright yellow to blue (ca. 30 min). The solvent was evaporated to dryness (70 mmHg, 25°C), and the resulting blue solid was dissolved in water (5 ml) and submitted to a flash gel permeation column chromatography using Sephadex LH-20 as stationary phase and water as eluent (1.5 cm × 20 cm, 20 psi). Dark bluish-purple fractions were combined and lyophilized (−80°C, 0.08 mbar). BeetBlue was obtained in 70% yield and kept as a solid [melting point (m.p.), 251°C/decomp] at −20°C. The purity of BeetBlue samples was verified by analytical reversed-phase high-performance liquid chromatography (HPLC) before use.

High-resolution mass spectrometry (HRMS) [ESI(+)-TOF] calculated for $C_{15}H_{17}N_2\ O_4^+(m/z)$: $[M + H]^+$, 289.1183; found, 289.1181; difference, 0.69 parts per million (ppm) (Fig. 1D and fig. S7).

^{1}H NMR (800 MHz, D_2O, δ): 7.51 (d, J = 15.1 Hz, 1H), 6.64 (d, J = 15.1 Hz, 1H), 6.46 (s, 1H), 6.09 (s, 1H), 4.43 (dd, J = 6.7, 8.4 Hz, 1H), 3.38 (dd, J = 17.7, 6.7 Hz, 1H), 3.16 (dd, J = 17.7, 8.4 Hz, 1H), 2.32 (s, 3H), and 2.24 (s, 3H) (fig. S1).

^{13}C NMR (200 MHz, D_2O, δ): 177.99, 168.01, 164.87, 162.04, 146.60, 135.25, 131.90, 119.96, 117.25, 117.24, 111.29, 56.95, 29.82, 15.65, and 13.76 (fig. S2).

Ultraviolet-visible (UV-vis)/Fl: λ_{abs}^{max} = 582 nm (water; Fig. 2A), λ_{Fl}^{max} = 623 nm (water, λ_{exc} = 570 nm), and $\varepsilon^{582nm} = 5.4 \times 10^4$ liter mol^{-1} cm^{-1} (water) (fig. S8).

Mass spectrometry

HPLC-HRMS data were acquired in a Shimadzu Prominence liquid chromatograph coupled to a Bruker Daltonics microTOF-QII mass spectrometer equipped with an electrospray source. BeetBlue was analyzed with a Luna C18(2) column (150 mm by 2 mm, 3 µm; Phenomenex) at 0.2 ml min^{-1} and 30°C under a linear gradient from 5 to 95% B in 15 min [solvent A, water; solvent B, acetonitrile; both containing 0.05% (v/v) formic acid].

Absorption and emission spectra

UV-Vis absorption spectra were acquired on a Varian Cary 50 Bio spectrophotometer equipped with a Peltier thermostated cell holder.

Fluorescence emission spectra were recorded using a Varian Eclipse spectrometer attached to a thermostatic bath. All spectrophotometric measurements were carried out at 25° ± 1°C using a 10-mm optical path (o.p.) quartz cuvette, unless otherwise stated.

Color analyses

Color analyses were performed using the CIE D65 at 10° using the Color software (Agilent). The values u′ and the v′ were obtained in a Varian Cary 50 Bio spectrophotometer equipped with a Peltier thermostated cell holder at 25° ± 1°C. Solutions of BeetBlue (10 μM) were prepared in acidified methanol (MeOH), water (W), dimethyl sulfoxide (DMSO), trifluoroethanol (TFE), isopropanol (iPrOH), and hexafluoro-2-propanol (HFIP).

Photobleaching assay

A solution of BeetBlue in water with an absorbance of 1.0 (1.85×10^{-5} M) was placed in a fluorescence quartz cuvette with an internal volume of 1500 μl (10 × 4–mm o.p., 119F, Hellma) and irradiated at 355 or 582 nm under magnetic stirring for 2 hours (4-mm o.p.). Excitation at 582 nm was carried out using a Quantel Nd:YAG/OPO Rainbow laser system (89 mW, 10-Hz pulse frequency, 4- to 8-ns pulse width, 5- to 6-mm pulse diameter). Excitation at 355 nm was carried out using a CryLas FTSS 355-Q3 solid state laser (0.7 mW, 1-kHz pulse frequency, 1.1-ns pulse width, 0.15- to 0.25-mm pulse diameter). Solutions were kept at room temperature, and the absorption spectrum was registered from 300 to 800 nm (10-mm o.p.) at every 15 min.

Cell viability

Flow cytometry

The cell viability assay was carried out using the human epithelial cell line ARPE-19. The cells were cultured in complete media Dulbecco's modified Eagle's medium (DMEM)/F12 containing 10% of fetal bovine serum until confluence. A cell density of 1×10^6 cells ml^{-1} was used in the incubation step with BeetBlue (10 μM) and phosphate-buffered saline [PBS; 10 mM (pH 7.4)] for 24 hours and hydrogen peroxide (50 mM) for 5 hours. During the incubation time, ARPE-19 was maintained at room temperature, protected from light, and stirred using a rotating shaker. The suspension of cells was centrifuged and washed twice with PBS. Cell viability was determined by flow cytometry performed by BD FACSCanto II. The experiment was carried out for each sample labeled with 7-AAD (0.25 μg per 10^6 cells) and recorded using the channel PerCP-Cy5.5 (670-nm-long pass filter).

MTT assay

HepaRG, Hep-G2, and Huh-7 cell lines were cultured in DMEM containing 10% of fetal bovine serum until confluence. Cells were seeded in a 96-well plate (1×10^4 cells per well) and treated with BeetBlue (millimolar to nanomolar concentration range) or submitted to UVC radiation (positive control, 20 or 50 J/m^2) for up to 8 hours. MTT solution in PBS [10% (v/v) of 5 mg ml^{-1}) was added to the medium. After incubation (37°C for 1 hour), the medium was removed, and 200 μl of DMSO was added into each well. The absorption of the resulting purple solution was measured at 570 nm. Three independent experiments were performed for each treatment.

Comet assay

HepaRG cells were seeded in a 24-well plate (1.8×10^5 cells per well) and treated with BeetBlue (1×10^{-5} M) for up to 8 hours or submitted to UVC irradiation at a dose of 6 J/m^2. After the treatment, cells were removed from the plate by trypsinization and immediately mixed with 0.5% (w/v) low-melting agarose at 37°C. The mixture was spread on microscope slides pretreated with a thin layer of 1.5% (w/v) agarose; proteins and cellular membranes were removed by incubation in lysis solution at 4°C for 24 hours. The slides were exposed to alkaline buffer [300 mM NaOH and 1 mM EDTA in water (pH > 13) for 30 min] and subjected to electrophoresis (25 V cm^{-1} and 300 mA for 30 min). Next, the slides were rinsed with neutralization buffer [0.4 M tris buffer (pH 7.5)], dried, and fixed using 99% ethanol for 5 min (*40*). Cell nucleus was stained with ethidium bromide (20 μg ml^{-1}) and analyzed with a fluorescence microscope (Olympus BX51, green filter set) using the Komet 6.0 software. Results of the DNA fragmentation were expressed as the olive tail moment (OTM). Hundred tail moments were analyzed in duplicate for each group in a total of three independent experiments. Untreated cells were used as a negative control group.

Zebrafish toxicity

Zebrafish toxicity assay was carried out based on OECD no. 236 Guideline on Fish Embryo Acute Toxicity Test (*34*). Egg collection achieved the validation criteria for fertilization rate (≥70%) and the development stage up to 90 min after fertilization. In a 24-well plate, 20 embryos were distributed in four wells containing 2 ml of BeetBlue (10 μM) in E2 media. Control embryos were maintained in E2 media only. The microplate was kept at 28°C in an incubator for 96 hours, and every 24 hours, observations such as coagulated embryos, lack of heartbeat, nondetachment of the tail, and lack of somite formation were recorded as indicators of lethality. All values are expressed as means ± SD of eight replicates from two independent experiments. Statistical data analysis was performed by one-way analysis of variance (ANOVA). The level of statistical significance was taken to be $P < 0.05$. The protocols for manipulating zebrafish used in this work were evaluated and approved by the Animal Use and Ethic Committee (CEUAIB, Comitê de Ética no Uso de Animais do Instituto Butantan) of the Instituto Butantan (Protocol 1270/14). They are in accordance with Colégio Brasileiro de Experimentação Animal (COBEA) guidelines and the National law for Laboratory Animal Experimentation (Law No. 11.794, 8 October 2008).

Computational methods

Ground state geometries were optimized without constraints in water at the density functional theory (DFT) SMD/B3LYP/6-31+G(d,p) level. Stationary points were characterized as minima by vibrational analysis. Linear optical properties were calculated using single-point energy calculations at the time-dependent (TD)–DFT SMD/PBE0/6-31+G(d,p)level. Geometry optimization and TD-DFT calculations were carried out using the Gaussian 09 rev. D.01 software package (*41*). The electron excitation analysis and NTO calculations were carried out using the Multiwfn software (*42*). ^{1}H chemical shifts were calculated using the GIAO method at the SMD(H2O)/WP04/aug-cc-pVDZ level (*43*) using a scaling factor of 31.9153 ppm (*44*).

SUPPLEMENTARY MATERIALS

Supplementary material for this article is available at http://advances.sciencemag.org/cgi/content/full/6/14/eaaz0421/DC1

View/request a protocol for this paper from *Bio-protocol*.

REFERENCES AND NOTES

1. B. R. Conway, S. Chatterjee, G. D. Field, G. D. Horwitz, E. N. Johnson, K. Koida, K. Mancuso, Advances in color science: From retina to behavior. *J. Neurosci.* **30**, 14955–14963 (2010).

2. J. Sun, B. Bhushan, J. Tong, Structural coloration in nature. *RSC Adv.* **3**, 14862–14889 (2013).
3. A. Fleiss, K. S. Sarkisyan, A brief review of bioluminescent systems (2019). *Curr. Genet.* **65**, 877–882 (2019).
4. A. G. Newsome, C. A. Culver, R. B. van Breemen, Nature's palette: The search for natural blue colorants. *J. Agric. Food Chem.* **62**, 6498–6511 (2014).
5. M. Buchweitz, Natural solutions for blue colors in food, in *Handbook on Natural Pigments in Food and Beverages,* R. Carle, R. M. Schweiggert, Eds. (Woodhead Publishing, Cambridge, ed. 1, 2016), chap. 17, pp. 355–384.
6. T. Coultate, R. S. Blackburn, Food colorants: Their past, present and future. *Color. Technol.* **134**, 165–186 (2018).
7. K. Kupferschmidt, In search of blue. *Science* **364**, 424–429 (2019).
8. A. E. Smith, H. Mizoguchi, K. Delaney, N. A. Spaldin, A. W. Sleight, M. A. Subramanian, Mn^{3+} in trigonal bipyramidal coordination: A new blue chromophore. *J. Am. Chem. Soc.* **131**, 17084–17086 (2009).
9. M. Casutt, B. Dittmar, H. Makowska, T. Marszalek, S. Kushida, U. H. F. Bunz, J. Freudenberg, D. Jänsch, K. Müllen, A diketopyrrolopyrrole-based dimer as a blue pigment. *Chem. Eur. J* **25**, 2723–2728 (2019).
10. G. Gottsberger, O. R. Gottlieb, Blue flower pigmentation and evolutionary advancement. *Biochem. Syst. Ecol.* **9**, 13–18 (1981).
11. K. Yoshida, M. Mori, T. Kondo, Blue flower color development by anthocyanins: From chemical structure to cell physiology. *Nat. Prod. Rep.* **26**, 884–915 (2009).
12. J. Mendoza, N. Basílio, F. Pina, T. Kondo, K. Yoshida, Rationalizing the color in heavenly blue anthocyanin: A complete kinetic and thermodynamic study. *J. Phys. Chem. B* **122**, 4982–4992 (2018).
13. X. Li, F. Siddique, G. T. M. Silva, F. H. Quina, H. Lischka, A. J. A. Aquino, Quantum chemical evidence for the origin of the red/blue colors of *Hydrangea macrophylla* sepals. *New J. Chem.* **43**, 7532–7540 (2019).
14. K. M. Davies, Swapping one red pigment for another. *Nat. Genet.* **47**, 5–6 (2015).
15. A. Osbourn, Painting with betalains. *Nat. Plants* **3**, 852–853 (2017).
16. G. T. Sigurdson, P. Tang, M. M. Giusti, Natural colorants: Food colorants from natural sources. *Annu. Rev. Food Sci. Technol.* **8**, 261–280 (2017).
17. M. V. Pavliuk, A. M. Cieślak, M. Abdellah, A. Budinská, S. Pullen, K. Sokołowski, D. L. A. Fernandes, J. Szlachetko, E. L. Bastos, S. Ott, L. Hammarström, T. Edvinsson, J. Lewiński, J. Sá, Hydrogen evolution with nanoengineered ZnO interfaces decorated using a beetroot extract and a hydrogenase mimic. *Sustain. Energ. Fuels* **1**, 69–73 (2017).
18. M. V. Pavliuk, A. B. Fernandes, M. Abdellah, D. L. A. Fernandes, C. O. Machado, I. Rocha, Y. Hattori, C. Paun, E. L. Bastos, J. Sá, Nano-hybrid plasmonic photocatalyst for hydrogen production at 20% efficiency. *Sci. Rep.* **7**, 8670 (2017).
19. F. Gandía-Herrero, J. Escribano, F. García-Carmona, Purification and antiradical properties of the structural unit of betalains. *J. Nat. Prod.* **75**, 1030–1036 (2012).
20. W. Schliemann, N. Kobayashi, D. Strack, The decisive step in betaxanthin biosynthesis is a spontaneous reaction. *Plant Physiol.* **119**, 1217–1232 (1999).
21. A. C. B. Rodrigues, I. de Fátima Afonso Mariz, E. M. S. Maçoas, R. R. Tonelli, J. M. G. Martinho, F. H. Quina, E. L. Bastos, Bioinspired water-soluble two-photon fluorophores. *Dyes Pigm.* **150**, 105–111 (2018).
22. L. C. P. Gonçalves, N. B. Lopes, F. A. Augusto, R. M. Pioli, C. O. Machado, B. C. Freitas-Dörr, H. B. Suffredini, E. L. Bastos, Phenolic betalain as antioxidants: *Meta* means more. *Pure Appl. Chem.* **92**, 243–253 (2020).
23. K. K. Nakashima, E. L. Bastos, Rationale on the high radical scavenging capacity of betalains. *Antioxidants* **8**, E222 (2019).
24. P.-A. Girod, J.-P. Zryd, Biogenesis of betalains: Purification and partial characterization of dopa 4,5-dioxygenase from *amanita-muscaria*. *Phytochemistry* **30**, 169–174 (1991).
25. W. Schliemann, U. Steiner, D. Strack, Betanidin formation from dihydroxyphenylalanine in a model assay system. *Phytochemistry* **49**, 1593–1598 (1998).
26. P. S. Grewal, C. Modavi, Z. N. Russ, N. C. Harris, J. E. Dueber, Bioproduction of a betalain color palette in *Saccharomyces cerevisiae*. *Metab. Eng.* **45**, 180–188 (2018).
27. M. A. Guerrero-Rubio, R. López-Llorca, P. Henarejos-Escudero, F. García-Carmona, F. Gandía-Herrero, Scaled-up biotechnological production of individual betalains in a microbial system. *Microb. Biotechnol.* **12**, 993–1002 (2019).
28. F. C. Stintzing, J. Conrad, I. Klaiber, U. Beifuss, R. Carle, Structural investigations on betacyanin pigments by LC NMR and 2D NMR spectroscopy. *Phytochemistry* **65**, 415–422 (2004).
29. F. C. Stintzing, F. Kugler, R. Carle, J. Conrad, First ^{13}C-NMR assignments of betaxanthins. *Helv. Chim. Acta* **89**, 1008–1016 (2006).
30. F. Gandía-Herrero, J. Escribano, F. García-Carmona, Structural implications on color, fluorescence, and antiradical activity in betalains. *Planta* **232**, 449–460 (2010).
31. J. M. Wolfe, T. S. Horowitz, What attributes guide the deployment of visual attention and how do they do it? *Nat. Rev. Neurosci.* **5**, 495–501 (2004).
32. M. T. Donato, R. Jover, M. J. Gómez-Lechón, Hepatic cell lines for drug hepatotoxicity testing: Limitations and strategies to upgrade their metabolic competence by gene engineering. *Curr. Drug Metab.* **14**, 946–968 (2013).
33. D. Awad, J. Wilińska, D. Gousia, X. Shi, J. Eddous, A. Müller, V. Wagner, C. Hillner, W. Brannath, A. Mohr, D. Gabel, Toxicity and phototoxicity in human ARPE-19 retinal pigment epithelium cells of dyes commonly used in retinal surgery. *Eur. J. Ophthalmol.* **28**, 433–440 (2018).
34. M. Sobanska, S. Scholz, A.-M. Nyman, R. Cesnaitis, S. Gutierrez Alonso, N. Klüver, R. Kühne, H. Tyle, J. de Knecht, Z. Dang, I. Lundbergh, C. Carlon, W. De Coen, Applicability of the fish embryo acute toxicity (FET) test (OECD 236) in the regulatory context of registration, evaluation, authorisation, and restriction of chemicals (REACH). *Environ. Toxicol. Chem.* **37**, 657–670 (2018).
35. P. Di Mascio, G. R. Martinez, S. Miyamoto, G. E. Ronsein, M. H. G. Medeiros, J. Cadet, Singlet Molecular Oxygen Reactions with Nucleic Acids, Lipids, and Proteins. *Chem. Rev.* **119**, 2043–2086 (2019).
36. S. Nizioński, M. Wendel, M. F. Rode, D. Prukała, M. Sikorski, S. Wybraniec, G. Burdziński, Photophysical properties of betaxanthins: Miraxanthin V - insight into the excited-state deactivation mechanism from experiment and computations. *RSC Adv.* **7**, 6411–6421 (2017).
37. M. Wendel, S. Nizinski, D. Prukala, M. Sikorski, S. Wybraniec, G. Burdzinski, Ultrafast internal conversion in neobetanin in comparison to betacyanins. *J. Photochem. Photobiol. A* **332**, 602–610 (2017).
38. H. V. Kiefer, E. Gruber, J. Langeland, P. A. Kusochek, A. V. Bochenkova, L. H. Andersen, Intrinsic photoisomerization dynamics of protonated schiff-base retinal. *Nat. Commun.* **10**, 1210 (2019).
39. Z. Yaqoob, E. J. McDowell, J. Wu, X. Heng, J. P. Fingler, C. Yang, Molecular contrast optical coherence tomography: A pump-probe scheme using indocyanine green as a contrast agent. *J. Biomed. Opt.* **11**, 054017 (2006).
40. Y. T. Magalhães, J. O. Farias, L. F. Monteiro, F. L. Forti, Measuring the contributions of the rho pathway to the DNA damage response in tumor epithelial cells. *Methods Mol. Biol.* **1821**, 339–355 (2018).
41. M. J. Frisch, G. W. Trucks, H. B. Schlegel, G. E. Scuseria, M. A. Robb, J. R. Cheeseman, G. Scalmani, V. Barone, G. A. Petersson, H. Nakatsuji, X. Li, M. Caricato, A. Marenich, J. Bloino, B. G. Janesko, R. Gomperts, B. Mennucci, H. P. Hratchian, J. V. Ortiz, A. F. Izmaylov, J. L. Sonnenberg, D. Williams-Young, F. Ding, F. Lipparini, F. Egidi, J. Goings, B. Peng, A. Petrone, T. Henderson, D. Ranasinghe, V. G. Zakrzewski, J. Gao, N. Rega, G. Zheng, W. Liang, M. Hada, M. Ehara, K. Toyota, R. Fukuda, J. Hasegawa, M. Ishida, T. Nakajima, Y. Honda, O. Kitao, H. Nakai, T. Vreven, K. Throssell, J. A. Montgomery, Jr., J. E. Peralta, F. Ogliaro, M. Bearpark, J. J. Heyd, E. Brothers, K. N. Kudin, V. N. Staroverov, T. Keith, R. Kobayashi, J. Normand, K. Raghavachari, A. Rendell, J. C. Burant, S. S. Iyengar, J. Tomasi, M. Cossi, J. M. Millam, M. Klene, C. Adamo, R. Cammi, J. W. Ochterski, R. L. Martin, K. Morokuma, O. Farkas, J. B. Foresman, D. J. Fox Gaussian 09, revision D.01 (Gaussian Inc., 2009).
42. T. Lu, F. Chen, Multiwfn: A multifunctional wavefunction analyzer. *J. Comput. Chem.* **33**, 580–592 (2012).
43. K. W. Wiitala, T. R. Hoye, C. J. Cramer, Hybrid density functional methods empirically optimized for the computation of ^{13}C and ^{1}H chemical shifts in chloroform solution. *J. Chem. Theory Comput.* **2**, 1085–1092 (2006).
44. G. K. Pierens, ^{1}H and ^{13}C NMR scaling factors for the calculation of chemical shifts in commonly used solvents using density functional theory. *J. Comput. Chem.* **35**, 1388–1394 (2014).

Acknowledgments: We thank J. D. Vilcachagua (Analytical Central, IQUSP) for help with the NMR analyses, H. C. Junqueira and M. Baptista for the assistance in the photochemical studies, and M. H. G. de Medeiros for making the microscope available to us. We dedicate this work in memory of Ahmed "Nabil" Abdellah Qenawy. **Funding:** This work was supported by São Paulo Research Foundation–FAPESP (2014/22136-4, 2016/21445-9, and 2019/06391-8 to E.L.B.; 2014/10563-5 to B.C.F.-D.; 2015/24760-0 to C.O.M.; 2015/18474-4 to A.C.M.; 2018/25842-8 to L.C.P.G.; and 2015/25629-4 to A.B.F.), the Brazilian National Council for Scientific and Technological Development–CNPq (303341/2016-5 to E.L.B.), and the Coordenação de Aperfeiçoamento de Pessoal de Nível Superior (CAPES, Finance Code 001). **Author contributions:** E.L.B. conceived the study. E.L.B., L.C.P.G., and J.S. wrote the paper. E.L.B., B.C.F.-D., F.A.D., M.L.-F., F.L.F., L.C.R., and J.S. designed the experiments. B.C.F.-D., C.O.M., A.C.P., E.L.B., M.A., A.B.F., F.L.F., L.C.R., and F.A.D. performed the experimental work. E.L.B. carried out theoretical calculations. All authors discussed and interpreted the results. **Competing interests:** The authors declare that they have no competing interests. **Data and materials availability:** All data needed to evaluate the conclusions in the paper are present in the paper and/or the Supplementary Materials. Additional data related to this paper may be requested from the authors.

Submitted 7 August 2019
Accepted 9 January 2020
Published 3 April 2020
10.1126/sciadv.aaz0421

Citation: B. C. Freitas-Dörr, C. O. Machado, A. C. Pinheiro, A. B. Fernandes, F. A. Dörr, E. Pinto, M. Lopes-Ferreira, M. Abdellah, J. Sá, L. C. Russo, F. L. Forti, L. C. P. Gonçalves, E. L. Bastos, A metal-free blue chromophore derived from plant pigments. *Sci. Adv.* **6**, eaaz0421 (2020).

Science Advances

A metal-free blue chromophore derived from plant pigments

B. C. Freitas-Dörr, C. O. Machado, A. C. Pinheiro, A. B. Fernandes, F. A. Dörr, E. Pinto, M. Lopes-Ferreira, M. Abdellah, J. Sá, L. C. Russo, F. L. Forti, L. C. P. Gonçalves and E. L. Bastos

Sci Adv **6** (14), eaaz0421.
DOI: 10.1126/sciadv.aaz0421